International Journal of Engineering Research & Technology (IJERT)
ISSN: 2278-0181
Vol. 4 Issue 02, February-2015

Comparison of the Electrical and Thermal Performances of a PV Sensor for Covered and Uncovered with a Glass

Abidi Sihem[1*], Sammouda Habib[1]
[1] LabEM, LR11ES34- Université de Sousse, Ecole Supérieure des Sciences et de Technologie, Rue Amin ElAbbassi, 4011 Hammam Sousse (Tunisie)

Bennacer Rachid[2]
[2] ENS-Cachan, LMT, Dpt GC 61, Av. Président Wilson 94235 Cachan Cedex, France

***Abstract*— A thermal model regarding a photovoltaic module has been developed and validated using experimental data. The aim of this study is to recover heat wasted by Joule effect by adding the heat exchanger rear sensor and an additional window forward. We will also compare the thermal and electric performance a hybrid sensor covered with an additional pane with another uncovered in order to improve the efficiency of the sensor and the influence of air flows and then we will study the effect of the thermal conductivity of the metallic absorber on the most optimal system performance. The results showed that key design parameters such as the heat flux captured, air flows, and the thermal conductivity of the solid absorber had a significant influence on both the electrical and thermal efficiency of the hybrid sensor.**

Keywords*— Convection; Heat Exchanger; Sensor Solar PV cells; Coolant

I. INTRODUCTION

Solar energy is distinguished from other resource-based carbon, low pollution and sustainable availability. Every day the sun sends to the earth more energy than the 6 billion inhabitants of the planet consume in 25 years. This resource is inexhaustible on a human scale; however, it is still largely untapped. But the PV cells presented some drawbacks such as the heating of the cell temperature junction and the low PV sensors yield (20 %).

Koyunbaba Basak et al. [1] presented a comparison of Trombe wall system between a single glass PV panel and another with a double glass. After validation of the numerical models with the experimental results, these systems will be used in a building in different climatic conditions, glass types and thermal masses. Furthermore, they noted that the temperature reached by PV cells is higher than the ambient temperature and that the efficiency of PVTs is greater than the combined sum of separate PV and thermal collectors. In the light of this, they suggest that PVT systems offer a cost effective solution for applications where roof area is limited. Kamthania et al. [2] evaluated the performance of a hybrid PVT double pass facade for space heating in the composite climate of New Delhi by using a semi transparent PV module. Thermal modelling has been carried out based on the first and second law of thermodynamics in order to estimate the electrical and thermal energy along with the exergy for a "semi transparent" hybrid PVT double pass façade instead of an opaque PV panel. In the light of this, they suggested that the semi transparent PV module has more electrical efficiency than the opaque PV module. Sarhaddi et al. [3] evaluated the exergetic performance of a solar PV/T air collector and carried out the detailed energy and exergy analysis to calculate the thermal and electrical parameters, exergy components and exergy efficiency of a typical PV/T air collector. Caluianu et al. [4] developed and validated, using experimental data, a BP 585 F photovoltaic panel thermal model. They made a simulation by applying the Galerkin finite element method to the flow and energy equations, incorporating an implicit convective boundary condition. The values of the root mean square error and the correlation coefficient between the experimental and the simulated values of the panel temperature show a good accuracy of the model. Afterwards, this was used to simulate the convective flow between the photovoltaic module and the roof wall. The influence of this channel width was then studied. Velocity and temperature variations were calculated at the beginning, the middle and the exit of the channel for 10 mm, 20 mm and 30 mm width. Ibrahim et al. [5] made the comparison of the device between each type of the flat plate PV/T collectors and performance of each of them. Besides that, this paper provides reviews of the latest development and the future work on the PV/T collector based on previous researcher's review. This work also convoluted the principal classifications of flat plate PVT collectors systems. This classification provides clearly how this flat plat PV/T collector system designed can be grouped systematically according to the type of working fluid used such as water or air. An interesting attempt has been made by Anderson et al. [6] to integrate the PV/T system to a building. In this experiment, PV cells are laid onto a standing seam or troughed sheet roof using a laminated technique to a BIPVT system. The designed BIPVT system allowed the water to pass through underneath the cells to generate hot water when exposed to the heat from the sun. The result from this experiment showed that the design parameters included the fin, the conductivity between the cells, the roofing material and also the laminating technique influenced the BIPVT

system. They strongly believed that the BIPVT could be made cheaper even when using a common pre-coated colour steel material. Jin et al. [7] developed an experiment on a single-pass PV/T with a rectangular tunnel absorber. The rectangular tunnel which acted as an absorber collector has been fixed underneath the photovoltaic panel. The main purpose of the experiment is to identify a suitable air flow for cooling the PV panel. By doing this, the efficiency of the panel will increase. The result showed that the combined PV/T efficiency was 64.72% and the thermal efficiency at 54.70% with solar irradiance of 817.4Wm^{-2}, and the mass flow rate reached 0.0287kgs^{-1} at ambient temperature of 25°C. They concluded that the hybrid PV/T with a rectangular tunnel as a heat absorber showed a higher performance compared to the conventional PV/T system. Bolcken et al. [8] and Defraeye et al. [9] verified the importance of near-wall modelling for CHTC prediction at building surface and reported overestimations with standard and non-equilibrium wall functions (WF) that can be up to 60% and 30%, respectively. For the windward façade of a cubic building, they did not resolve the viscous sub-layer and the buffer layer (where the largest resistance to surface heat and mass transfer is embedded). Karava et al. [10] developed accurate thermal analysis models for the design and control of building-integrated Photovoltaic/Thermal (PV/T) systems. Since the convective heat transfer between the roof and the external airflow has a significant impact on the electrical and thermal efficiency of the system. The main objective of this paper is to evaluate the CHTC for the inclined roof surfaces of low-rise buildings. Specifically, the aim is to develop, for the first time, dimensionless correlations for the CHTC that take into account the effects of the building/roof geometry and the incident atmospheric boundary layers on the roof velocity and thermal boundary layers, notably the terrain roughness length and the turbulence intensity at eaves height. Daghigh et al. [11] presented the more detailed studies of a new design of an absorber collector under the meteorological conditions of Malaysia (hot and humid climate). Since few studies of BIPVT water based systems especially amorphous silicon systems have been conducted up to now, therefore further experimental and numerical work should be carried out aiming at incrementing our knowledge regarding improving electrical performance and thermal efficiency of PV/T solar collector using a new design of absorber collector. In the work of Ibrahim et al. [12], seven configurations of new sensors absorption PV/T were designed, investigated and compared. Simulations were performed to determine the best absorber design that gives the highest efficiency (total efficiency). In these simulations, the system was analysed with various parameters, such as solar radiation, ambient temperature, and flow rate conditions. It was assumed that the collector was represented as a flat thermal collector with a single glazing sheet. Based on these simulations, spiral flow design proved to be the best design with the highest thermal efficiency of 50.12% and a corresponding cell efficiency of 11.98%. Roman and Tiwari [13, 14] studied the annual thermal and exergy efficiency of the PVT/a collector for five different Indian climate conditions. It was observed that the exergy efficiency is 40-45% lower than the thermal efficiency under strong solar radiation. Also the double-pass design shows a better performance than the single-pass option. Dubey et al. [15] studied different configurations of glass-to-glass and glass-to-tedlar PV modules. Analytical expressions for electrical efficiency with and without airflow were developed as a function of climatic and collector design parameters. Experiments at the Indian institute of technology, Delhi found that the glass-to-glass type is able to achieve a higher supply of air temperature and electrical efficiency. This is because the radiation that falls on the non-packing area of the glass-to-glass module is transmitted through the front cover. It's average PV efficiencies with and without duct were determined 10.4% and 9.75%, respectively. Hence, a difference of about 0.7% is obtained. The percentage differences between the PV efficiency of the glass-to-glass and that of the glass-to-tedlar type were respectively, 0.24% with duct and 0.086% without duct. In Hong Kong, Chow et al. [16] carried out outdoor measurements on two identical sheet-and-tube thermosyphon PVT/w collector systems, in which one was glazed. Together with a validated numerical model, the appropriateness of having front glazing was evaluated. The first law of thermodynamic evaluation indicates that the glazed design is always suitable whether the thermal or the overall energy output is to be maximised, but the exergy analysis supports the use of unglazed design if the increase of PV cell efficiency, packing factor, ratio of water mass to collector area and wind velocity are seen as desirable factors.

The objective of our work is to study the effect of an additional pane on the thermal performance, the influence of air flows. Then we will study the effect of the thermal conductivity of the metallic absorber on the most optimal system performance. Thus, we study the efficiency of the overall system using steady values of characteristic numbers, ***Ra***, heat flux captured, ***Re***, air flows, and $\boldsymbol{\lambda}$, the thermal conductivity of the solid absorber. This system is made up of a cavity of length H in direction z and width L so that aspect ratio A=L/H, enclosing a first coolant fluid with an open channel and a second driving coolant (air), the wall adjacent to the cavity is an absorber solid of high thermal conductivity. Above this system, we add an additional pane, as shown schematically in Fig.1.

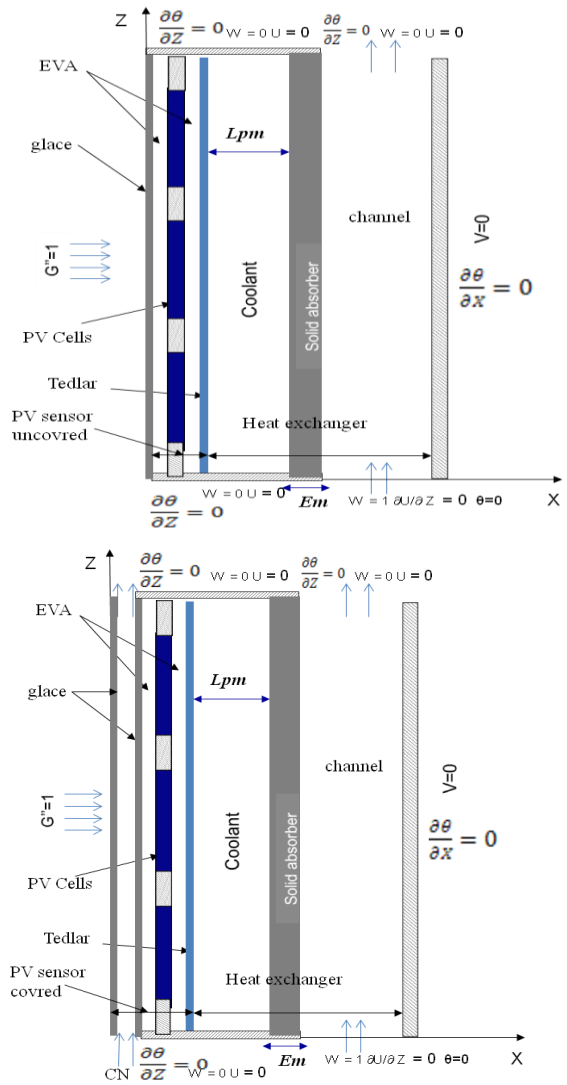

Fig. 1 Evolution of PV sensor configurations associated to heat exchanger: uncovered (a) and covered (b)

II. GOVERNING EQUATIONS

The movement of the fluids and their temperature are governed by continuity, momentum and energy equations in the solid and fluid phases. The heat flux imposed on the up boundary is considered only on the level of PV cells, with density q. Thus, the reference variables for length, velocity and temperature are chosen respectively as:

$X = \frac{x}{H}$and $Z = \frac{z}{H}$, $V_{ref} = \frac{\vartheta}{H}$ as diffusive velocity and $\Delta T = \frac{q_0}{\lambda} H$.

The dimensionless variables are: the temperature $\theta = \frac{T - T_a}{\Delta T}$ and velocity $\vec{V}(U,W)$.

The dimensionless conservation equations of mass and momentum of compressible fluid (air, coolant), in permanent regime, are:

- Navier-Stokes equations :

$$\vec{\nabla}.\vec{V} = 0 \qquad (1)$$

- Natural convection

$$(\vec{V}.\vec{\nabla}).\vec{V} = -\vec{\nabla}P + Gr\theta\overrightarrow{e_g} + \Delta\overrightarrow{V} \qquad (2)$$

where $\overrightarrow{e_g} = -cos\alpha\vec{\imath} - sin\alpha\vec{\jmath}$

-Forced convection

$$(\vec{V}.\vec{\nabla}).\vec{V} = -\vec{\nabla}P + \frac{Gr}{Re^2}\theta\overrightarrow{e_g} + \Delta\overrightarrow{V} \qquad (3)$$

-Energy equation at each fluid phase:

-Natural convection

$$\vec{V}.\vec{\nabla}\theta_{fi} = \frac{1}{Pr}\vec{\nabla}.\vec{\nabla}\theta_{fi} + \frac{Bi_i}{Pr}\frac{1}{\Delta X}(\theta_{fi} - \theta_{si}) + \frac{Bi_j}{Pr}\frac{1}{\Delta X}(\theta_{fi} - \theta_{sj}) \qquad (4)$$

-Forced convection

$$\vec{V}.\vec{\nabla}\theta_{fi} = \frac{1}{PrRe}\vec{\nabla}.\vec{\nabla}\theta_{fi} + \frac{Bi_i}{PrRe}\frac{1}{\Delta X}(\theta_{fi} - \theta_{si}) + \frac{Bi_j}{PrRe}\frac{1}{\Delta X}(\theta_{fi} - \theta_{sj}) \qquad (5)$$

The above equations are related to the fluid.

Eq. (3) involves the temperature of the solid θ_s. Thus, an energy equation should be written to determine θ_s. This equation reads:

- On the level of each solid**:**

$$\vec{\nabla}.(\vec{\nabla}\theta_{si}) + \frac{Bi_i}{R_{\lambda_i}}\frac{1}{\Delta X}(\theta_{si} - \theta_{fi}) + \frac{Bi_j}{Pr}\frac{1}{\Delta X}(\theta_{si} - \theta_{fj}) + G\frac{1}{\Delta X} = 0 \qquad (6)$$

$$G = \tau_{si}[\alpha_{sj}]I\frac{H}{\Delta T\lambda_{sj}}$$

❖ *On the level of PV cells*:

$$\vec{\nabla}.(\vec{\nabla}\theta_c) + 2\frac{Bi_i}{R_{\lambda_i}}\frac{1}{\Delta X}(\theta_c - \theta_{fi}) + (E - G)\frac{1}{\Delta X} = 0 \qquad (7)$$

Where E and G are the dimensionless quantity defined as:

$$E = \tau_{si}\beta_c(1 - \alpha_{si})\,\eta_{el}I\frac{1}{\Delta TLH\lambda_c}$$

$$G = \tau_{si}[\alpha_c\beta_c(1 - \alpha_{si})]I\frac{H}{\Delta T\lambda_c}$$

where τ, α, β_c and η_{el} are respectively transmittivity, absorptivity, packing factor and electrical efficiency.

The problem is characterized by the classical Prandtl number, Pr, the Rayleigh number, Ra, the Biot number of each fluid, $Bi_i = \frac{h_i H}{\lambda_i}$, which takes the value zero away from interfaces and the ratio of thermal conductivity $R_{\lambda_i} = \frac{\lambda_{si}}{\lambda_{fi}}$ with i and j, corresponding to nature of fluid and solid.

III. BOUNDARY CONDITIONS

The dimensionless boundary conditions are given by:

at X = 0 : W = 0, U = 0 and $\frac{\partial\theta}{\partial X} = 1$ at $(0 \le Z \le 1)$ (solar heat flow)

at X =A: W = 0, U = 0 and $\frac{\partial\theta}{\partial X} = 0$ at $(0 \le Z \le 1)$ (adiabatic)

at Z = 0 : $\frac{\partial W}{\partial Z} = 0$, $\frac{\partial U}{\partial Z} = 0$ et $\theta = 0$, at channel of double glass $(0 \le X \le 0.1)$ and W = 0, U = 0 and $\frac{\partial\theta}{\partial Z} = 0$, at the cavity $(0.1 \le X \le 0.6)$ and $W = 1$, $\frac{\partial U}{\partial Z} = 0$ et $\theta = 0$, at the channel $(0.6 \le X \le 1)$

at Z = 1 : $\frac{\partial W}{\partial Z} = 0$, $\frac{\partial U}{\partial Z} = 0$ and $\frac{\partial \theta}{\partial Z} = 0$, at the channel ($0 \le X \le 0.1$ and $0.6 \le X \le 1$) and W=0, U=0 and $\frac{\partial \theta}{\partial Z} = 0$, at the cavity ($0.1 \le X \le 0.6$)

IV. RESULTS AND DISCUSSION

The governing (Eqs. 1-7) with the boundary conditions were solved using the control finite volume method. The computational domain is divided into rectangular control volumes with one grid point located at the centre of the control volume that forms a basic cell. The set of conservation equations are integrated over the control volumes, leading to a balance equation for the fluxes at the interfaces. A second order scheme is used to discrete the equations; the false transient procedure is used in order to obtain a permanent solution. For faster convergence the SIMPLER algorithm, originally developed by Patankar [17], is coupled with the SIMPLEC algorithm by Van Doormaal and Raithby [18]. Non uniform grids are used in the program, allowing fine grid spacing near the boundaries. Trial calculations were necessary to optimize the computation time and accuracy. Convergence with the mesh size was verified by employing coarser and finer grids on selected test problems. The convergence criterion is based on both maximum error of continuity equation and the average quadratic residual over the whole domain for each equation was less than a prescribed value ζ (generally less than 10^{-6}).

The objective of our work is to study the effect of the additional pane on the thermal performance and the influence of air flows. Then we will investigate the effect of the thermal conductivity of the metallic absorber on the most optimal system performance. Thus, we evaluate the heat quantity transferred and the electrical and thermal efficiency defined as:

The heat quantity transferred, at position z, is calculated from the average Nusselt number, *Nu (z)*, a long x direction:

$$Nu(z) = \frac{1}{A}\int_0^A Nu(x,z)dx$$

and the average Nusselt number,

$$Nu = \int_0^1 Nu(z)dz$$

where $Nu(x,z) = -\left(\frac{\partial \theta(x,z)}{\partial x}\right) + W(x,z)\theta(x,z)$ the local heat transfer at any point.

-Electrical efficiency:

$$\eta_{el}(x,z) = 0.15(1-0.005\,\theta(x,z))$$

-Thermal efficiency:

$$\eta_{th}(x,z) = FR(\tau\alpha\beta_c + (1-\beta_c)\tau\alpha) - FR\,\theta(x,z)$$

where FR is the heat removal efficiency.

A. *Validation of numerical model:*

In order to obtain a grid independent solution, a grid refinement study is performed for three zones. Fig. 2 depicts the effect of the grid refinement on the global heat transfer flux (average Nusselt number, Nu). It is noted that the results are unchanged beyond (41*121) grid, we hence choose the (51,121) grid.

The precision of our results are evaluated by adapting our numerical model to Anderson et al. [6] system; Fig. 3 shows the variation of electrical (a) and thermal (b) efficiency with the ratio of the reduced temperature and global incident radiation on the collector surface.

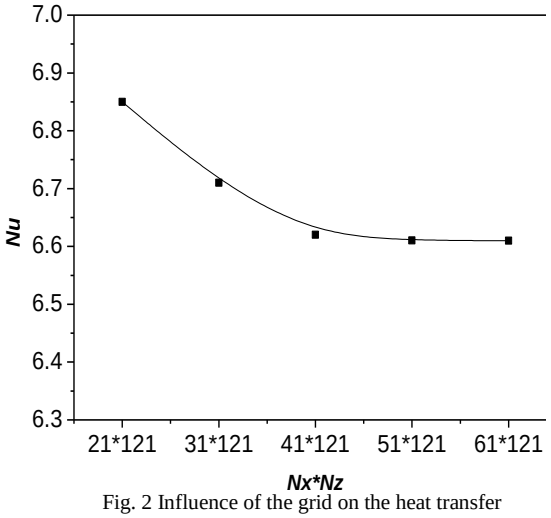

Fig. 2 Influence of the grid on the heat transfer

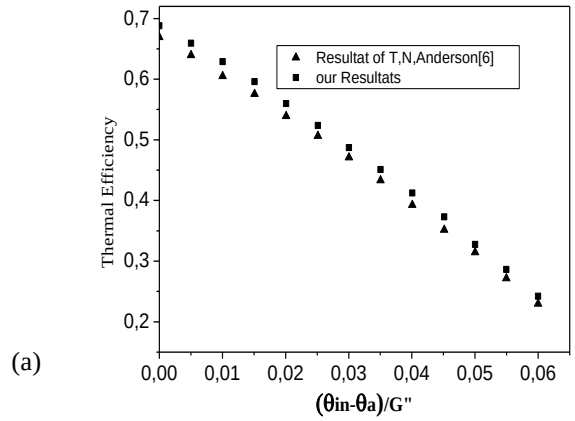

(a)

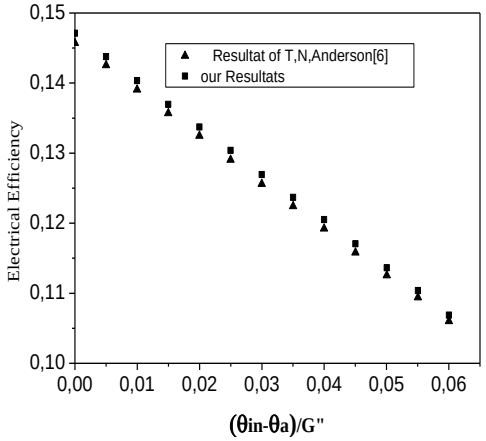

(b)

Fig. 3 Comparison of our results with those of T.N.Anderson et al. [6] for absorber conductivity, λ = 135W/mK

B. Parametric analysis:

- **Solar radiation effect**

Fig. 4 shows the evolution of the Nusselt number as a function of the heat flux received by the solar panel. When the solar heat flux through Rayleigh number ***Ra*** increases, the convective fluid flow progresses for both types of PVT sensor. Otherwise it is shown that when the PV sensor is covered, the heat transfer is enhanced. This can be explained by the fact that the metal interface does not transmit heat to the channel with the same proportion as that transmitted from the PV cells to the fluid in the area between the PV panel and the material.

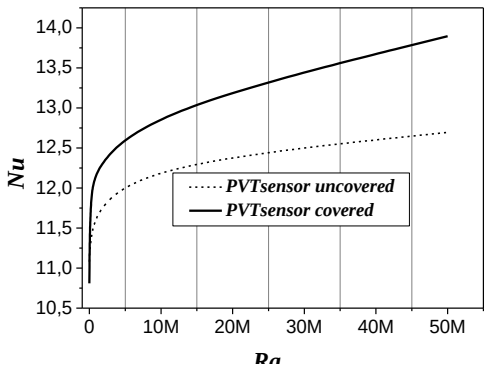

Fig. 4 Influence of the captured flux (ie Rayleigh number) on the thermal heat transfer: L_{pm} = 0.1, A = 1, Ra = 10^4, E_m = 0.1.

- **Regime flow effect, (injection speed)**

To improve the heat transfer between the solid exchanger and the channel, we increase the air injection speed through a ventilation system so that the forced convection is established in the channel. In the horizontal mid-plane, the profiles of the velocity vertical compound for different values of Reynolds number, Re, are shown in Fig. 5. It can be seen that the increasing ventilation has an influence on the velocity for both types of hybrid sensor PVT covered and uncovered with glass. Thus, the speed profiles illustrate the beginning of a boundary layer development at the level of channel input with optimal adjacent solid walls. Fig. 6 shows the temperature profiles at two remarkable positions: the median plane of the area between the PV panel and the material and the mid-plane of the channel for $\boldsymbol{Ra} = 10^4$, $\boldsymbol{L_{pm}}$=0.1, $\boldsymbol{E_m}$ = 0.1 and $\boldsymbol{A}$ = 1 and for different values of Reynolds number. We note that the effect of this parameter appears in both planes. Near the bottom wall of the photovoltaic panel (the plane of the area between the PV panel and material), one can observe that temperature at this area decreases by further augmenting Re value. In addition, we note that the temperature at the mid-plane of the channel increases when the Reynolds number increases. The air flow strengthens in the channel brings down the temperature level of operation of both types of hybrid sensor PVT covered and uncovered with glass. This can be explained by the fact that the increase of the air flow causes its rapid circulation and a rapid discharge of the heat towards the outside and thus a temperature lowering takes place.

- **Effect of the solid absorber thermal conductivity**

In what follows, we will investigate the effect of the thermal conductivity of the metallic absorber on the most optimal system performance: the PVT sensor covered with ventilation.

It can be seen from Fig. 7 (a) increasing the value of the heat transfer coefficient to 135 W/m^{2}K leads to improvement of the maximum thermal efficiency by almost 5%. Given that the high thermal conductivity adhesives are commonly used in attaching electrical components to heat sinks to improve cooling. It is evident that using them to attach the PV cells in the BIPVT would also improve the electrical efficiency. As illustrated at Fig. 7 (b), it can be seen that by reducing the bond thermal resistance, there is a marked increase in the electrical efficiency. As such, it would be more appropriate to ensure that the thermal conductivity between these bodies is maximised. However, it should also be recognised that these results are asymptotic, suggesting other areas that are limiting the efficiency of the BIPVT. In addition to improving the heat transfer between the absorber and the PV cells, we may improve the optical efficiency of the BIPVT system by reducing the reflectance of the PV cells.

V. CONCLUSION

To improve the performance of the hybrid photovoltaic/thermal system, a new heat exchanger of three coolants, two fluids and one solid, is associated with solar photovoltaic panel cells.

This exchanger consists of a cavity enclosing a first heat transfer fluid, and an open channel. The wall adjacent to the cavity is an absorber solid. The aim of our study is the comparison of the thermal and electric performance of a hybrid sensor covered with an additional pane and another uncovered in the aim of improving the efficiency of the sensor. The results show that adding the additional pane increases the temperature and thus the thermal performance of the hybrid PVT sensor is higher than that of the uncovered sensor. Results also show a high temperature level at the output of the sensor when the air velocity is low. For the same conditions, we found the lowest cell temperatures and therefore the greatest electrical efficiency of the sensor. It was demonstrated that the optimum performance of the system must be both electrical (junction temperature of the PV) and thermal (temperature of the hot air recovered at the outlet of the channel).

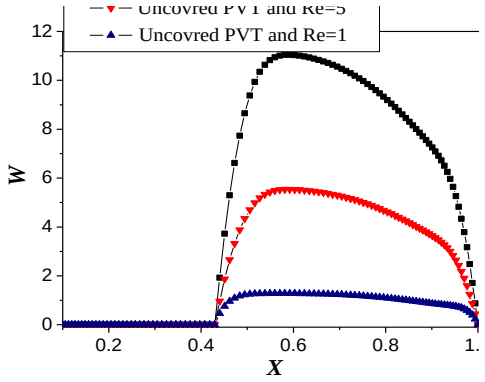

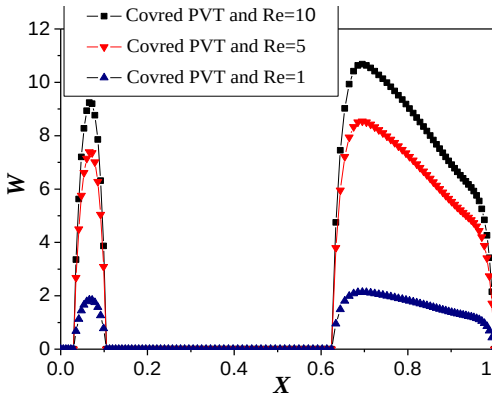

Fig. 5 Profiles of the vertical velocity component in the horizontal mid-plane with: Ra = 10^4, A = 1, L_{pm} = 0.1, E_m = 0.1 and for different Reynolds number (Re = 1 and 10) for PV sensor associated to heat exchanger and uncovered (covered) with glass

(a)

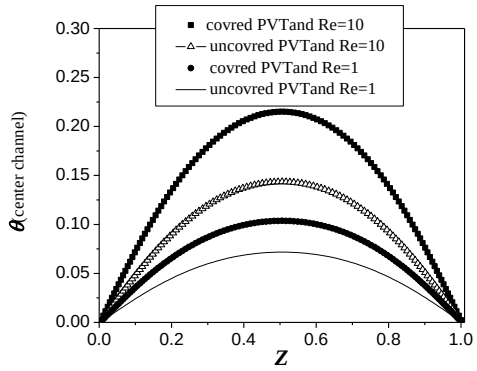

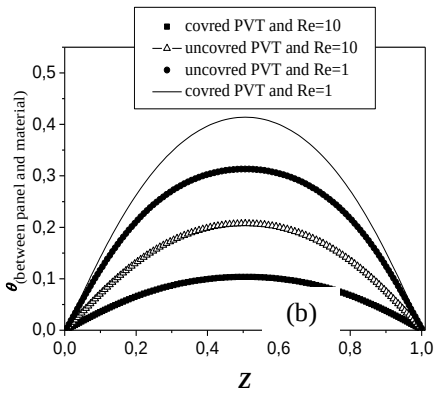

Fig. 6 Effect of the injection speed on the temperature profiles: (a) in the median plane of the channel and (b) between the PV panel and the material for Sensor PVT covered and uncovered with glass for: Ra = 10^4, A = 1, L_{pm} = 0.1, E_m = 0.1 and for different Reynolds number (Re = 1 and 10).

PV sensor associated to heat exchanger and uncovered with glass

PV sensor associated to heat exchanger and covered with glass

(a)

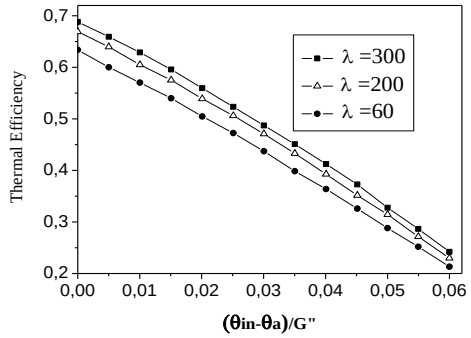

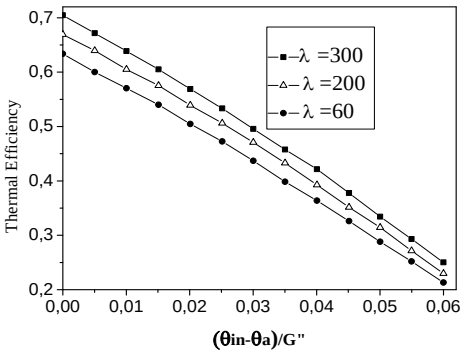

(b)

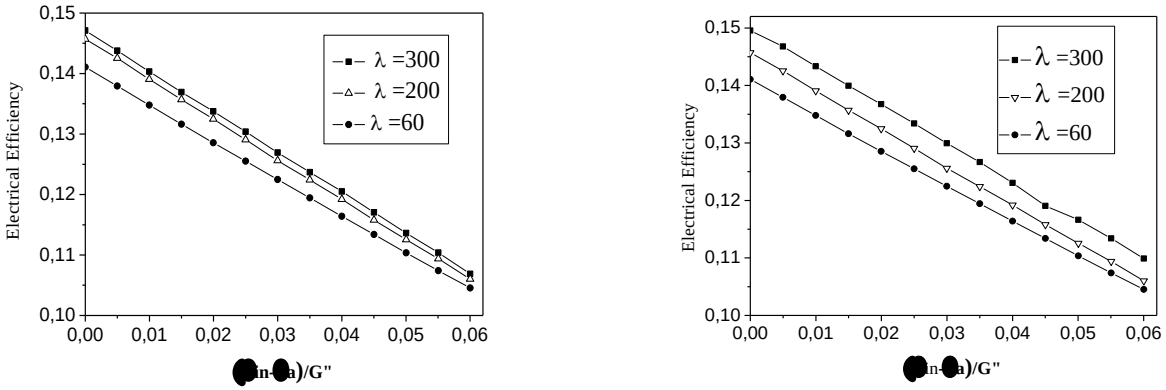

Fig. 7 Efficiency: (a) thermal and (b) electrical of system on the report of the reduce

REFERENCES

[1] Koyunbaba, B., Yilmaz, Z., (2012) The comparison of trombe wall systems with single glass, double glass and PV panels, Renewable Energy.. 45, 111-118.

[2] Kamthania, D., Nayak, S., Tiwari, G.N., (2011) Performance evaluation of a hybrid photovoltaic thermal double pass facade for space heating, Energy and Buildings., 43, 2274–2281.

[3] Sarhaddi, F., Farahat, S., Behzadmehr, A., (2010) Exergetic performance assessment pf a solar photovoltaic thermal (PV/T) air collector, Energy and Buildings., 42, 2184-2199.

[4] Caluianu, I.R., Baltaretu, F., (2012) Thermal modelling of a photovoltaic module under variable free convection conditions, Applied Thermal Engineering., 33-34, 86-91.

[5] Ibrahim, A., Othman, M. Y., Ruslan, M. H., Mat, S., Sopian, K., (2011) Recent advances in flat plate photovoltaic/ thermal (PV/T) solar collectors, Renewable and Sustainable Energy Reviews., 15, 352-365.

[6] Anderson, T.N., Duke, M., Morrison, G.L., Carson, J.K., (2009) Performance of a building integrated photovoltaic/thermal (BIPVT) solar collector, Solar Energy., 83, 445-455.

[7] Jin, GL., Ibrahim, A., Chean, YK., Daghigh, R., Ruslan, H., Mat, S., et al., (2010) Evaluation of single-pass photovoltaic-thermal air collector with rectangle tunnel absorber, A.J.of Applied Sciences., 7, 277-282.

[8] Blocken, B., Defraeye, T., Derome, D., Carmeliet, J., (2009) High-resolution CFD simulations for forced convective heat transfer coefficients at the façade of a low-rise building, Buildingand Environment., 44, 2396-2412.

[9] Defraeye, T., Blocken, B., Carmeliet, J., (2010) CFD analysis of convective heat transfer at the surfaces of a cube immersed in a turbulent boundary layer, I. J. of Heat and Mass transfer., 53, 297-308.

[10] Karava, P., Mohammad Jubayer, C., Savory, E., (2011) Numerical modelling of forced convective heat transfer from the inclined windward roof of an isolated low-rise building with application to photovoltaic/thermal systems, Applied Thermal Engineering., 31, 1950-1963.

[11] Daghigh, R., Ibrahim, A., Jin, GL., Ruslan, H., Sopian, K., (2011) Predicting the performance of amorphous and crystalline silicon based photovoltaic solar thermal collectors, Energy Conversion and Management., 52, 1741–1747.

[12] Ibrahim, A., Othman, MY., Ruslan, H., Alghoul, MA., Yahya, A., et al., (2009) Performance of photovoltaic thermal collector (PVT) with different absorbers design, WSEAS Trans Environ Develop., 5(3), 321–330.

[13] Roman, V., Tiwari, GN., (2008) Life cycle cost analysis of HPVT air collector under different Indian climatic conditions, Energy Policy., 36, 603-611.

[14] Roman, V., Tiwari, GN., (2009). A comparison study of energy and exergy performance of a hybrid photovoltaic double-pass and single-pass air collector, Int J Energy Res., 33, 605-617.

[15] Dubey, S., Sandhu, GS., Tiwari, GN., (2009) Analytical expression for electrical efficiency of PV/T hybrid air collector, Appl Energy., 86, 697-705.

[16] T Chow, T., Pei, G., Fong, KF., Lin, Z., Chan, ALS., Ji, J., (2009) Energy and exergy analysis of photovoltaic-thermal collector with and without glass cover, Applied Energy., 86(3), 310-6.

[17] Patankar, S.V. (1980) Numerical Heat Transfer and Fluid Flow. Hemisphere/McGraw-Hill, Washington, 1090-1093.

[18] Van Doormaal, J.P., Raithby, G.D., (1984) Enhancements of the simple Method for predicting incompressible fluid flows. Numerical HeatTransfer.,7,147-163.